Bifurcation transitions in gap-junction-coupled neurons

Annabelle Shaffer,[1] Allison L. Harris,[1] Rosangela Follmann,[2,1] and Epaminondas Rosa, Jr.[1,2]
[1]*Department of Physics, Illinois State University, Normal, Illinois 61790, USA*
[2]*School of Biological Sciences, Illinois State University, Normal, Illinois 61790, USA*
(Received 4 August 2016; published 3 October 2016)

Here we investigate transitions occurring in the dynamical states of pairs of distinct neurons electrically coupled, with one neuron tonic and the other bursting. Depending on the dynamics of the individual neurons, and for strong enough coupling, they synchronize either in a tonic or a bursting regime, or initially tonic transitioning to bursting via a period doubling cascade. Certain intrinsic properties of the individual neurons such as minimum firing rates are carried over into the dynamics of the coupled neurons affecting their ultimate synchronous state.

DOI: 10.1103/PhysRevE.94.042301

I. INTRODUCTION

A major feature of networked neurons is their capability for firing in synchrony. It allows them to collectively perform tasks that would otherwise be difficult to execute. Many examples of neurons spiking synchronously illustrate well the relevance of this operational functionality, including Hebbian learning and memory [1,2], wake-sleep cycles [3], and central pattern generators [4,5]. Synchronization has also been shown to be a critical component of neurological conditions such as epilepsy [6] and Parkinson's disease [7]. In particular, and of interest in this study, some neuronal synchronous states are associated with transitions between regimes of tonic (rhythmic single spiking) and of bursting (repeating sequences of multiple spikes) activity. Tonic-to-bursting transitions play important roles, for instance, in thalamocortical neurons at sleeping transition states [8], and in sensory-motor nuclei that generate the typical tremors in Parkinson's disease [9]. Several studies have investigated them, mostly involving individual dynamics of the neurons [10,11], but less is known about these transitions in the context of distinct interacting neurons.

Here we use numerical simulations to examine tonic-to-bursting transitions involving pairs of Hodgkin-Huxley-type neurons coupled via gap junctions. Physiologically, gap junctions are sets of channels connecting adjacent neurons permitting ions and electric impulses to pass through their joint membranes. Electrical connection through gap junctions can lead neurons into synchrony as well as influence chemical communication, and are thought to play an important part in brain development and pattern formation [12]. Our focus is on how the dynamical states of two different neurons, one tonic and the other bursting, evolve as the electrical coupling strength between them increases. Different outcomes are observed, depending on the initial dynamical states of the two neurons and on how strong the coupling between them is. We analyze three cases: (1) the two neurons first synchronize in the tonic regime and remain tonic, (2) the two neurons first synchronize in the tonic regime, then undergo a period-doubling cascade and traverse chaos into a continued bursting regime, and (3) the two neurons first synchronize in the bursting regime and remain bursting.

The single neuron model used here also experiences a tonic-to-bursting transition, albeit different from the transition found in this study of two coupled neurons. For the single neuron, as opposed to a period doubling cascade, it happens via period adding in the bursting states [13], with a minimum firing rate at the transition point between tonic and bursting. We found that this minimum firing rate seems to be carried over to the synchronous tonic-to-bursting transition that exists at the point of synchronization of the two neurons. We observed that for a particular linear combination of parameter values for the two neurons, one tonic and the other bursting, the synchronization occurs with a minimum coupling strength. Additionally, the synchronization between the two neurons also happens at a minimum firing rate that matches the minimum firing rate of the single neuron at its tonic-to-burst transition. In what follows we describe our findings indicating that certain individual neuron signatures are maintained in the collective of a network, potentially defining its overall behavior.

II. SINGLE NEURON DYNAMICS

A. Neuron model equations

The neuronal mathematical model we use here is based on the ground-breaking work of Alan Hodgkin and Andrew Huxley [14], explaining the ionic processes that underly initiation and propagation of action potentials in the giant axon of the squid. The model equations in this work were initially intended for studying thermo-sensitive neurons [15], and have since been applied to a variety of systems such as noisy ionic conductances [16], psychiatric disorders [17], stochastic dynamics [18], sleep-wake cycles [19], and inhibitory coupling in neurons [20]. The equations incorporate physiologically relevant properties of an excitable lipid bilayer cell membrane embedded with a variety of proteins, some of them working as ion channels, others as receptors and still others as transporters. The membrane separates the cell's inside medium from the outside, with both media exhibiting dynamical imbalances of ion concentrations. As an extension of the Hodgkin and Huxley equations, the Huber-Braun model neuron we use possesses dynamics of fast spiking and of slow subthreshold oscillations, both associated with sodium and potassium ion channels. Fast spiking results from the coordinated depolarizing sodium (I_d) and repolarizing potassium (I_r) currents. The subthreshold oscillations result from the slow depolarization sodium (I_{sd}) and slow repolarization calcium-dependent potassium currents (I_{sr}). Voltage and time dependent components are at the core of the model equations, with the membrane playing the role

of a capacitor being charged and discharged by a variety of currents dependent on conductances and driving forces.

The equation for the time evolution of the electric potential V across the membrane is then given by

$$C\dot{V} = -I_{\text{leak}} - I_{\text{Na}} - I_{\text{K}} - I_{\text{sd}} - I_{\text{sr}} - I_{\text{inj}}, \quad (1)$$

where C represents the membrane capacitance and, neglecting first approximation fluctuations, I_{inj} represents an external injected current therefore considered a control parameter, and may include the sum of all excitatory and inhibitory synaptic inputs. The leak current is represented by $I_{\text{leak}} = g_{\text{leak}}(V - V_{\text{leak}})$ where g_{leak} is the constant leak conductance and V_{leak} is the equilibrium potential. The fast and slow currents for sodium and potassium labeled Na, K, *sd,* and *sr*, respectively, are given by $I_{\text{j}} = \rho g_{\text{j}} a_{\text{j}}(V - V_{\text{j}})$ where j denotes Na^+, K^+, *sd*, or *sr*, V_{j} represents the equilibrium potential for each corresponding current, and ρ is a scaling parameter for temperature dependence (constant in this study). The maximum conductances and equilibrium potentials are represented by g_{j} and $V_{0\text{j}}$, respectively. The opening and closing of the ion channels are directly associated with characteristic time constants τ_{j}, which, in the case of sodium channels, are rather small. Sodium channels can thus be considered as activating instantaneously, with an activation function represented by $a_{\text{Na}} = \frac{1}{1+e^{-s_{\text{Na}}(V-V_{0_{\text{Na}}})}}$, where s_{Na} sets the slope of the sigmoid curve, and $V_{0_{\text{Na}}}$ corresponds to the half-activation potential. The equations for the other three activation variables are

$$\dot{a}_{\text{K}} = \frac{\phi}{\tau_{\text{K}}}(a_{\text{K}\infty} - a_{\text{K}}), \quad (2)$$

$$\dot{a}_{\text{sd}} = \frac{\phi}{\tau_{\text{sd}}}(a_{\text{sd}\infty} - a_{\text{sd}}), \quad (3)$$

$$\dot{a}_{\text{sr}} = -\frac{\phi}{\tau_{\text{sr}}}(\nu_{\text{acc}} I_{\text{sd}} + \nu_{\text{dep}} a_{\text{sr}}). \quad (4)$$

The scaling parameters for temperature dependencies, ρ and ϕ, are here set at the constant values $\rho = 0.607$ and $\phi = 0.124$. The activation functions $a_{\text{j}\infty}$ are represented by sigmoid steady state curves given by $a_{\text{j}\infty} = \frac{1}{1+e^{-s_{\text{j}}(V-V_{0\text{j}})}}$, j = K, *sd*, *sr*. In this model $a_{\text{Na}} \equiv a_{\text{Na}\infty}$, as a result of the very fast Na^+ channel activation, and Ca^{++} accumulation and depletion respectively included in ν_{acc} and ν_{dep}. Deactivation is embedded in the functional timing of the in-place activation functions and the corresponding conductances. Equations (1) through (4) can mimic a wide range of neuronal dynamics, with parameter values throughout this work as shown in the Appendix, unless otherwise explicitly mentioned in the text. In Sec. 3 we use these equations to represent two neurons connected via bidirectional electric coupling. In this case Eq. (1) has an addition current, $I_{0,1} = g_{\text{c}}(V_{0,1} - V_{1,0})$, where the subscripts refer to the two neurons named 0 and 1, and the conductance g_{c} is the coupling constant. The numerical simulations were carried out applying the standard Runge-Kutta fourth order method, and the variables and parameters in the model represent quantities of physiological relevance for the real system. This includes the conductance g_{c}, except that the behaviors we see in our study would be expected to be found at weaker coupling in the real system [21,22].

B. Calcium-activated potassium current

Essentially, action potentials are produced when open Na^+ channels allow enough flow of Na^+ into the cell, raising the membrane potential above the threshold of firing. Overlapping with the process of closing Na^+ channels, K^+ channels open but this time the flow of ions is in the opposite direction, from inside to outside of the cell. The overall result is that after the quick rise, the membrane potential decreases sharply, ending the action potential with a downward overshooting translated into hyperpolarization due to the concomitant inactivation of the Na^+ channels. The wake of the action potential may be followed by an extended phase controlled by K^+ channels activated by Ca^{++}.

These channels are important regulators for neuronal excitability, including pacemaker neurons in the hypothalamic arcuate nucleus [23], are believed to limit the neuron's firing rate and also to be responsible for spike-frequency adaptation [24–28]. The control parameter g_{sr} in our model equations represents the maximum conductance associated with K^+ channels activated by Ca^{++}. It is an important parameter used here in association with the injected current I_{inj} to generate a wide variety of spiking patterns as shown in Fig. 1, where the color (online) map in panel (a) displays colored (shades of gray) regions associated with different neural behaviors, as indicated by the points 1, 2, 3, and 4, corresponding respectively to panels (c) tonic, (d) bursting, (e) chaos, and (f) bursting with one spike per burst. The gray area on the upper right-hand side of panel (a) is for subthreshold oscillations only, with no spikes. Barely visible traces of green (light gray) correspond to parameter space regions for bursts with alternated two and three spikes (voltage trace not shown). In panel (a), the border between tonic [region

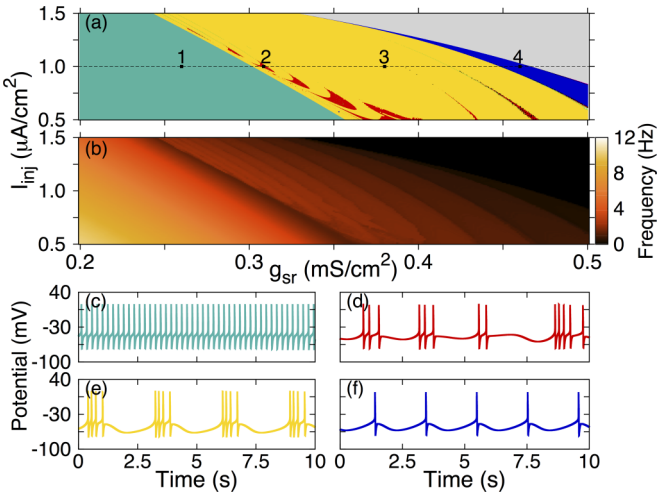

FIG. 1. Single neuron dynamics. (a) Color map for g_{sr} vs I_{inj} with colors (different shades of gray) related to the neuron's spiking patterns as depicted in panels (c), (d), (e), and (f) corresponding respectively to parameter space points 1, 2, 3, and 4 in panel (a). (b) Color map equivalent of parameter space of map in panel (a), for the corresponding firing rates according to the color coded bar on the right-hand side (dark to light gray). Voltage traces (c) tonic, (d) chaos, (e) burst with four spikes per burst, and (f) bursting with one spike per burst corresponding to points 1, 2, 3, and 4 respectively in panel (a).

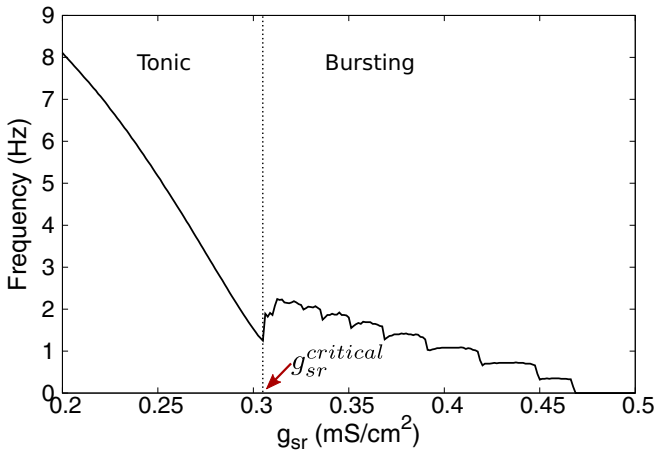

FIG. 2. Single neuron firing rate as a function of g_{sr} with $I_{inj} = 1.0$. The arrow indicates the critical value $g_{sr}^{critical} = 0.305$ were the transition between tonic and burst regimes occurs for the single neuron.

containing point 1, cyan (medium light gray)] and bursting [(region containing points 2 and 3, red and yellow (gray and light gray)] parameter spaces is of particular relevance because the transition between these two regions represents a drastic change in the dynamical state of the neuron, although not necessarily translating into big changes in its firing rate. As an agent for slow hyperpolarization of the cell membrane, increasing g_{sr} values should eventually make the tonic neuron go into the bursting regime.

Panel (b) shows the color (shades of gray) coded average firing rate (color bar on the right-hand side in Hertz) associated with each combination of g_{sr} and I_{inj} in panel (a). This color coded frequency shows how the firing rate varies in the range of g_{sr} and I_{inj} as displayed, indicating that the overall firing rate of the single neuron decreases with increasing values of g_{sr} and I_{inj}. All firing rates were obtained from long time averages of the corresponding simulated dynamics. An extended range of this color map can be found in Ref. [20].

For the purpose of this work we focus on fixed $I_{inj} = 1.0$ in order to study the interactions between tonic and bursting neurons electrically coupled. Along this $I_{inj} = 1.0$ line [dotted, shown in Fig. 1(a)], increasing values of g_{sr} make the neuron's firing rate evolve as displayed in Fig. 2, with two distinct overall downward trends. For g_{sr} values between 0.200 and 0.305 (units for conductances g assumed to be mS/cm^2 and for currents I to be μA/cm^2 throughout the text) the plot is smooth with a more accentuated slope compared to the bumpy, with a less accentuated slope for g_{sr} values between 0.305 and 0.500. In fact, the critical value $g_{sr}^{critical} = 0.305$ defines the transition point between tonic (to the left) and bursting (to the right) regimes along the $I_{inj} = 1.0$ line in Fig. 1(a).

In the tonic region, starting at $g_{sr} = 0.200$ mS/cm^2 with a frequency of $f = 8.11$ Hz, increasing values of g_{sr} up to $g_{sr}^{critical}$ lowers the neuron's frequency down to $f^{critical} = 1.25$ Hz, at which point for a short range of increasing g_{sr} up to the value 0.3125 actually raises the neuron's frequency to 2.125 Hz. This change in trend from lowering to increasing the neuron's frequency also marks the change in behavior of the neuron from tonic to bursting. As we shall see, this transition seems to play a role in the way two neurons, one tonic and the other bursting, synchronize in a common regime, either tonic or bursting. Continuing to increase g_{sr} sets the neuron on an upward trend in frequency until $g_{sr} \simeq 0.3125$ mS/cm^2 with a frequency $f = 2.24$ Hz. From this point on, increasing g_{sr} puts the neuron on an overall trend of decreasing frequency values, with a few bumps in a staircase format all the way through $g_{sr} \simeq 0.469$, where it enters a narrow band of subthreshold oscillations with no spikes, and then afterwards enters a region where it remains in its resting potential. Essentially, increasing g_{sr} corresponds to increasing the number of open calcium-dependent potassium channels, causing the membrane potential to move down toward repolarization, and therefore lowering the neuron's spiking frequency. Besides the tonic *vs*. burst behavior for the neuron in the respective ranges between 0.200 and 0.305, and between 0.305 and 0.46875, the rates of frequency change in the two regimes are drastically different as seen by the slopes of the plot in the two regions in addition to the smooth (tonic) versus bumpy (burst) evolutions. All the critical values of the parameters in this work were obtained from the data generated from our computer simulations.

III. ELECTRICALLY COUPLED NEURONS

A. Tonic versus bursting synchronization

Pairs of neurons hereafter named neuron 0 and neuron 1, electrically connected through diffusive coupling [29,30] $I_{0,1} = g_c(V_{0,1} - V_{1,0})$, may synchronize or not, depending on how different from each other the intrinsic dynamics of the individual neurons are, and on how strong the coupling g_c between them might be. For the purpose of this study we select neuron 0 to be tonic and neuron 1 to be bursting. Let us set neuron 0 with $g_{sr0} = 0.24$ [frequency $f_0 = 5.84$ Hz, voltage trace in red (gray) shown in Fig. 3 inset (a)] and neuron 1 with $g_{sr1} = 0.36$ [frequency $f_1 = 1.69$ Hz, voltage trace in

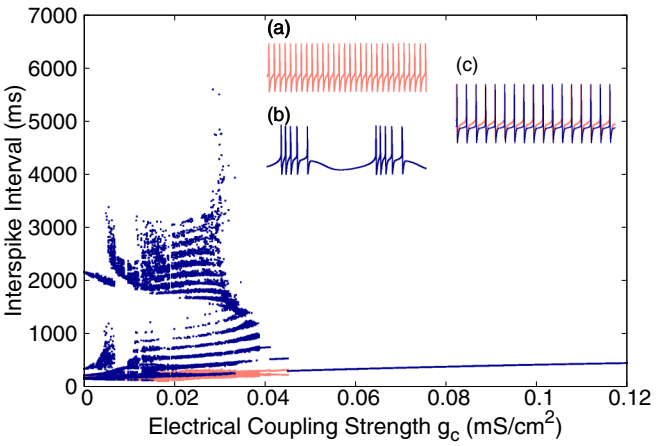

FIG. 3. Superimposed bifurcation diagrams for tonic [salmon (gray)] and bursting [dark blue (black)] neurons for increasing g_c. Their dynamical states evolve to synchrony in the tonic regime for $g_c \simeq 0.049$. Insets (a) and (b) display the voltage traces for uncoupled tonic neuron 0 [$g_{sr0} = 0.24$, salmon (gray)] and bursting neuron 1 [$g_{sr1} = 0.38$, dark blue (black)], respectively. Inset (c) shows the superimposed voltage traces of the synchronized neurons.

blue (black) shown in Fig. 3 inset (b)]. Their superimposed bifurcation diagrams keeping the same coded colors and using the electrical coupling strength g_c as the bifurcation parameter, are shown in Fig. 3.

For $g_c = 0$, the two neurons are in their original states which start to change as g_c begins to increase. Neuron 0 has its initially fixed interspike interval varying in a small range while neuron 1 goes from its original five spikes per burst state to states of larger numbers of spikes per burst as indicated by the stripes (each stripe roughly representing an interspike interval in the respective burst). At $g_c \simeq 0.030$, the bursting neuron 1 undergoes a typical homoclinic bifurcation that happens when a periodic orbit collides with a saddle point [31]. Past the homoclinic bifurcation point the magnitude of the interspike intervals for neuron 1 decreases sharply and at $g_c \simeq 0.045$ the two neurons synchronize in a period-one state remaining so from that point on (voltage traces of the two neurons shown superimposed in inset (c)). In this case, $g_{sr0} = 0.24$ to the left and $g_{sr1} = 0.36$ to the right are positioned at about equal distances from $g_{sr}^{critical} = 0.305$ (see Fig. 2). However, they correspond to very disparate firing rates, $f_0 = 5.84$ Hz and $f_1 = 1.69$ Hz, due to rather different slopes for the firing rate versus g_{sr} curves for tonic and bursting regimes displayed in Fig. 2. This means that the tonic neuron 0 is firing at a rate about three and a half times the firing rate of the bursting neuron 1, making neuron 0 more dominant. The tendency would be for these two neurons to synchronize in the tonic regime, and indeed this is what they do, remaining so for the extent of the range of the coupling strength.

Let us now look at another case of two neurons initially uncoupled, neuron 0 with $g_{sr0} = 0.29$ [frequency $f_0 = 2.22$ Hz, voltage trace shown in Fig. 4 inset (a)] and neuron 1 with $g_{sr1} = 0.41$ [frequency $f_1 = 1.08$ Hz, voltage trace shown in Fig. 4 inset (b)], both at $I_{inj} = 1.0$. Similar to the previous case depicted in Fig. 3, here the superimposed bifurcation diagrams (Fig. 4) start at $g_c = 0$ with neuron 0 (red) tonic and neuron 1 (blue) bursting. Increasing the value of g_c initially allows the two neurons to evolve separately, passing through a few transitions including windows of periodicity and also a homoclinic bifurcation (at $g_c \simeq 0.018$), continuing up to $g_c \simeq 0.048$ at which point they synchronize. However, different from the previous case, they now synchronize in the bursting regime. Their superimposed voltage traces are shown in Fig. 4 inset (c).

The $g_{sr0} = 0.29$ and $g_{sr1} = 0.41$ values in this case are not nearly equidistant, respectively to the left and to the right, from $g_{sr}^{critical} = 0.305$. In fact, the value of g_{sr0} is much closer to $g_{sr}^{critical}$ than that of g_{sr1}, putting neuron 0 closer to the transition point between tonic and bursting compared with the position of neuron 1. Despite the frequency of neuron 0 to be about twice that of neuron 1, the strong busting dynamics of neuron 1 is the predominant factor, forcing the tonic neuron 0 into bursting when they synchronize.

The two cases presented above suggest that knowledge about the initial states of the two neurons may not be sufficient to anticipate the regime in which they will eventually synchronize. Moreover, a higher initial firing rate displayed by either of the initially uncoupled neurons is not guaranteed to make their common synchronous state that of the faster neuron.

An additional measure that can help to better understand the tonic versus bursting synchronization dichotomy takes into account the frequency the two neurons share when they first synchronize. The color map of Fig. 5, with g_{sr0} values for neuron 0 along the x axis and g_{sr1} values for neuron 1 along the y axis, shows the firing rate of the two neurons at the point where they synchronize, quantified in the color code indicated by the color bar on the right-hand side of the figure. Consider, for example, a point at the bottom left corner of this color map with coordinates $g_{sr0} = 0.21$ for neuron 0, originally tonic, and $g_{sr1} = 0.32$ for neuron 1, originally bursting. With a

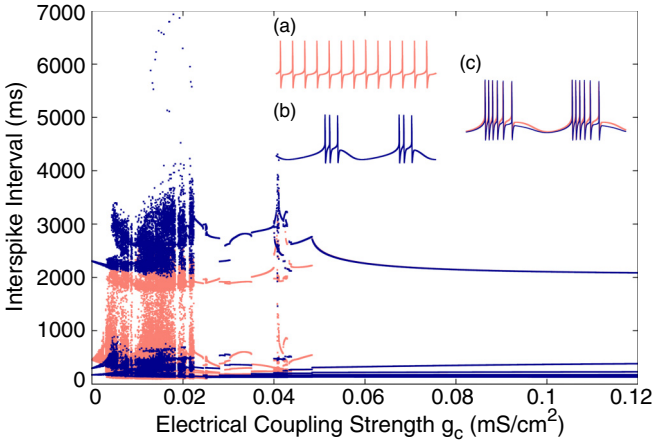

FIG. 4. Superimposed bifurcation diagrams for tonic [salmon (gray)] and bursting [dark blue (black)] neurons for increasing g_c. Their dynamical states evolve to synchrony in the bursting regime for $g_c \simeq 0.048$. Insets (a) and (b) display the traces for uncoupled tonic neuron 0 [$g_{sr0} = 0.29$, salmon (gray)] and bursting neuron 1 [$g_{sr1} = 0.41$, dark blue (black)] respectively. Inset (c) shows the superimposed traces of the synchronized neurons in the tonic regime.

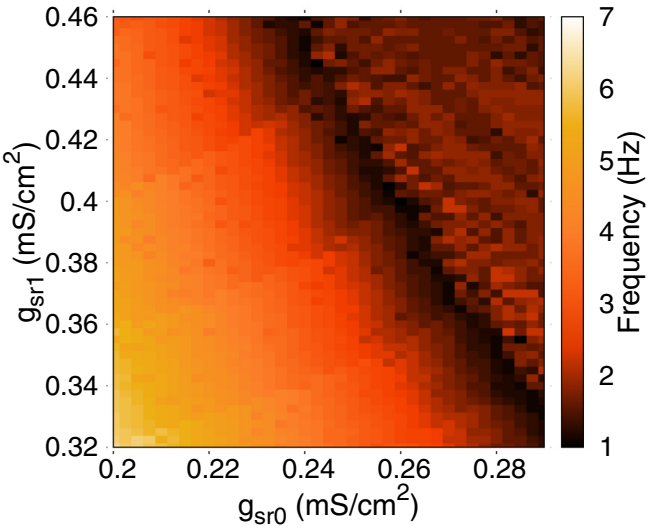

FIG. 5. Parameter space color map for different values of g_{sr0} and g_{sr1}. The color code (bar indicated on the right-hand side, black to light gray) shows the firing rate at which the two coupled neurons synchronize. The black strip marks the border between neurons synchronized in the tonic regime (on the left) and bursting regime (on the right). The firing rate along this border is $f_{min} = 1.25$ Hz.

strong enough coupling, they synchronize in the tonic regime with a common firing rate of $f_{0\text{sync}} = f_{1\text{sync}} = 5.80$ Hz.

Consider now a point at the top right corner, with coordinates $g_{\text{sr0}} = 0.28$ for neuron 0 originally tonic, and $g_{\text{sr1}} = 0.44$ for neuron 1 originally bursting. When they first synchronize they do so in the bursting regime, with a common firing rate of $f_{0\text{sync}} = f_{1\text{sync}} = 1.8$ Hz. If we start at the first point on the bottom left corner and move in parameter space on a straight line to the second point on the top right corner, our starting point is in a region of higher synchronous frequency f_{sync}, and as we move toward the top right corner of the map, f_{sync} initially decreases until we reach a region with the lowest frequency (black strip with negative slope). Past the darker strip we enter a region of increasing f_{sync}, but now the firing rate is going up at a slower pace compared with the decrease in the fire rate encountered on the left-hand side of the black strip. This strip of lowest f_{sync} happens to be at the border between the parameter space region for tonic synchronous states and the parameter space region for bursting synchronous states. This means that points in Fig. 5 to the left side of this border correspond to pairs of neurons, one tonic and the other bursting, that will synchronize in the tonic regime, and points on the right side of this border to neurons that will synchronize in the bursting regime. Moreover, the minimum synchronous frequency characteristic of the borderline points, typically $f_{\text{min}} = 1.25$ Hz, matches the minimum frequency characteristic of the single neuron, itself at the border between tonic and bursting states, with $g_{\text{sr}} = g_{\text{sr}}^{\text{critical}}$, as shown in Fig. 2. It seems that the two synchronous neurons acting as one, since they are operating synchronously, develop an peculiar combination of their individual dynamics that brings to their collective behavior characteristic features of their behaviors individually. In this way, the single-neuron graph showing the evolution of the firing rate as a function of the conductance g_{sr} in Fig. 2 can be viewed as a one-dimensional projection of the two-neuron color map in Fig. 5. Both display a minimum firing rate, f^{critical} for the single neuron and f_{sync} for the pairs of neurons, with the same value of 1.25 Hz, and both display distinct regions of tonic and of bursting regimes, separated by a point in the single neuron case and by a line in the pair of neurons case.

B. Bifurcation transitions

In the previous section we considered two cases for pairs of different electrically coupled neurons, one tonic, the other bursting. In the first case the neurons synchronize in the tonic regime, and in the second case the neurons synchronize in the bursting regime. We now discuss a third case, also for two electrically coupled neurons, one tonic and the other bursting, that incorporates aspects of both previous cases. This particular class of pairs of neurons first synchronize in the tonic regime and, as the coupling strength increases, the synchronous neurons undergo a transition through a period doubling cascade, then into chaotic behavior after which they reach the bursting regime where they remain from that point on.

In fact, the region in Fig. 5 above described as the parameter space area for which the two neurons synchronize in the tonic regime, can be split into two subregions, both for the two neurons first synchronizing in the tonic regime. However, as shown in Fig. 6, in parameter space labeled (i), the two neurons

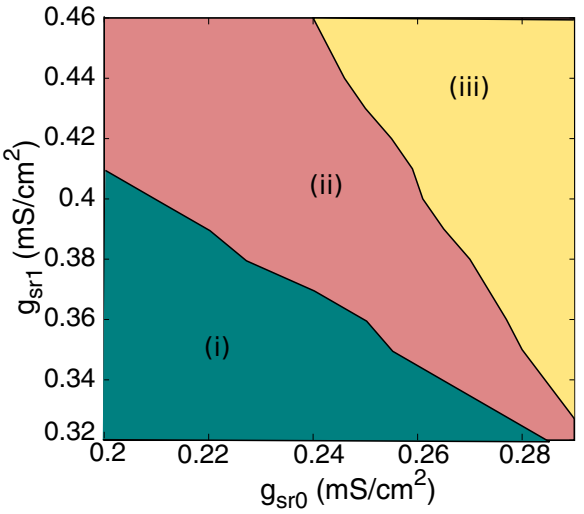

FIG. 6. Phase diagram for different values of g_{sr0} and g_{sr1} showing regions of (i) tonic, (ii) period-doubling cascade, and (iii) bursting behaviors.

synchronize in the tonic regime and remain in that state for increasing values of g_{sr}, while in parameter space labeled (ii), the two neurons first synchronize in the tonic regime and then, with increasing values of g_{sr} they move into chaos, then period-doubling cascade and then into bursting. In parameter space labeled (iii), the two neurons first synchronize in the bursting regime directly and stay in that state. The border line separating subregions (ii) and (iii) coincides with the dark points for lowest synchronous frequencies exhibited in Fig. 5.

In order to learn more about the evolution of the dynamics of two neurons with g_{sr} values intersecting in the subregion (ii) of Fig. 6, we couple neuron 0 with $g_{\text{sr0}} = 0.26$ initially tonic and neuron 1 with $g_{\text{sr1}} = 0.36$ initially bursting, and increase g_{c} from zero up to 0.14. The superimposed bifurcation diagrams

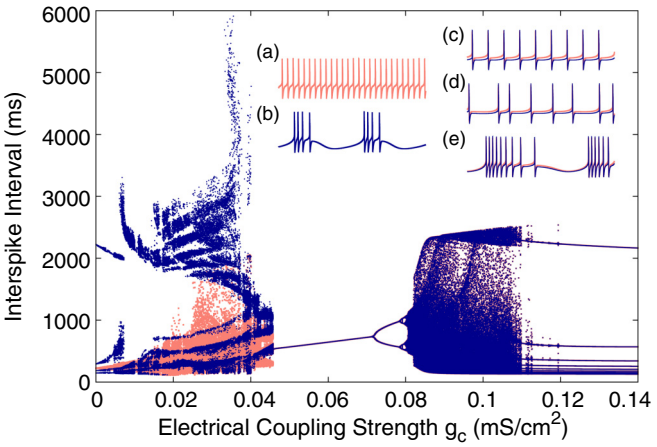

FIG. 7. Superimposed bifurcation diagrams for tonic [$g_{\text{sr0}} = 0.26$, salmon (gray), inset (a)] and bursting [$g_{\text{sr0}} = 0.38$, dark blue (black), inset (b)] coupled neurons for increasing g_{c}. Their dynamical states evolve to synchrony in the tonic regime for $g_{\text{c}} \simeq 0.046$, inset (c) for $g_{\text{c}} = 0.06$. Further increase in g_{c} leads the two synchronous neurons into a period-doubling cascade at $g_{\text{c}} \simeq 0.071$, to chaos [inset (d) for $g_{\text{c}} = 0.09$], and further down into bursting starting at $g_{\text{c}} \simeq 0.119$ [inset (e) for $g_{\text{c}} = 0.13$].

for the interspike intervals of neuron 0 and neuron 1, using g_c as bifurcation parameter, is shown in Fig. 7 (neuron 0 red, neuron 1 blue). The two neurons start at their own (periodic) states at $g_c = 0$, and increasing g_c values initially expands the interspike intervals for both neurons in different ways.

In the g_c range between $\simeq$0.0024 and $\simeq$0.046 the two neurons remain nonsynchronous and mostly chaotic, except for a few windows of periodicity. By $g_c \simeq 0.046$ the two neurons synchronize in a period-one orbit which doubles at $g_c \simeq 0.071$, with another period-doubling at $g_c \simeq 0.079$, etc. It is a typical period-doubling cascade leading the two coupled neurons together into chaos, which happens at $g_c \simeq 0.0801$. Further increase in the values of g_c leads the synchronous neurons into chaos in the g_c range between $\simeq$0.081 and $\simeq$0.112 with several periodic windows opened by a saddle-node bifurcation and closed by a global bifurcation (internal crisis) [32]. At $g_c \simeq 0.112$ the two neurons leave the chaotic window and start into the bursting regime, with a few escapes up to $g_c \simeq 0.119$ from which point on the two neurons keep a solid bursting.

IV. CONCLUDING REMARKS

Synchronization in neurological systems is critical for the survival of many species. Networks of neurons precluded from operating in synchrony may jeopardize vital functions, underscoring the functional relevance of stable and robust mechanisms underlying neuronal synchronous processes. A commonly found way neurons use for communicating with one another is through gap junctions, implemented in this study to help unravel the intricacies involved in the achievement and maintaining of synchronous states. In particular, we are interested in better understanding processes leading pairs of reciprocally coupled neurons into one of two possible final states, tonic or bursting, or a transitional combination of both. The pair of neurons we use consists of one neuron initially in the tonic regime and the other initially in the bursting regime. As their coupling strength g_c is increased, the two neurons eventually synchronize either in the tonic or in the bursting state, depending on the values of their conductance g_{sr} associated with calcium dependent potassium channels. Three cases are distinguished: (i) The neurons synchronize in the tonic regime and remain so for the range of g_c; (ii) The neurons synchronize initially in the tonic regime and, as g_c increases, they go through a period-doubling cascade and then chaos, to ultimately reach the bursting state where they remain; (iii) The neurons synchronize in the bursting regime where they stay for the range of g_c (Fig. 6).

We found a direct connection between these synchronous (tonic and bursting) states for pairs of coupled neurons and the evolution of a single neuron from tonic to bursting with varying g_{sr}. For the single neuron, the transition between tonic and bursting happens for $g_{sr}^{\text{critical}} = 0.305$ at a lowest firing rate, $f_{\min} = 1.25$ Hz (Fig. 2, arrow). This frequency matches the minimum firing rate observed for pairs of coupled synchronous neurons as indicated by the black strip observed in Fig. 5. In the g_{sr0} range between 0.24 and 0.29, the combination of g_{sr0} and g_{sr1} values, that correspond to the common synchronous minimum firing rate for the two neurons, is represented by the linear relationship $g_{sr1} \simeq 1.03$–$2.40 g_{sr0}$, which is the line separating regions of tonic-to-bursting (ii) and bursting (iii) in Fig. 6. In addition, these g_{sr0} and g_{sr1} also correspond to the minimum g_c needed to synchronize the two neurons. Regions (i) and (ii) correspond both to first synchrony in the tonic regime. In (i) the two neurons synchronize first in the tonic regime and stay in that state, while in (ii) the two neurons also synchronize in the tonic regime but, for increasing g_c values, the two neurons move together to a period-doubling cascade, then to chaos, and finally to bursting where they stay. This shows the relevance of the conductance for potassium calcium-regulated channels, not only for influencing the dynamics of the single neuron, but also for the role it plays when coupled neurons move into synchronous states. For example, in Fig. 5 we plot the frequencies at which the two neurons first synchronize upon strong enough coupling. The range for g_{sr0} sets neuron 0 tonic, and the range for g_{sr1} sets neuron 1 bursting. Given the complexity of the reciprocal electrical interactions between the two different neurons, it is interesting that the relationship between the g_{sr} values for the two neurons is linear for the minimal synchronous frequency. On the other hand, back to Fig. 2, it should be expected that approaching g_{sr}^{critical} from the tonic side (increasing g_{sr} for the tonic neuron), and approaching the same g_{sr}^{critical} from the bursting side (decreasing g_{sr} for the bursting neuron), would set pairs of neurons with the tendency for synchronizing (with a common firing rate), therefore the negative slope for the black strip at $f_{\min}$ in Fig. 5.

An important problem still open involves the capability for prediction of the final state in which the two neurons will eventually synchronize, given a certain coupling strength between them. Our results suggest that, in the case of a tonic and a bursting neuron, there might exist a simple linear relationship between common parameters with the potential for providing a good indication of the final state.

ACKNOWLEDGMENTS

We thank Wolfgang Stein and Ed Ott for helpful discussions. This work was supported by a research grant from the Illinois State University College of Arts and Sciences.

APPENDIX: MODEL PARAMETERS

$$
\begin{aligned}
g_{\text{leak}} &= 0.1\,\text{mS/cm}^2, \quad V_{\text{leak}} = -60\,\text{mV},\\
g_{\text{Na}} &= 1.5\,\text{mS/cm}^2, \quad V_{\text{Na}} = 50\,\text{mV}, \quad V_{0\text{Na}} = -25\,\text{mV},\\
g_{\text{K}} &= 2.0\,\text{mS/cm}^2, \quad V_{\text{K}} = -90\,\text{mV}, \quad V_{0\text{K}} = -25\,\text{mV},\\
g_{\text{sd}} &= 0.25\,\text{mS/cm}^2, \quad V_{\text{sd}} = 50\,\text{mV}, \quad V_{0\text{sd}} = -40\,\text{mV},\\
g_{\text{sr}} &= 0.25\,\text{mS/cm}^2, \quad V_{\text{sr}} = -90\,\text{mV}, \quad C = 1\,\mu\text{F/cm}^2,\\
\tau_{\text{K}} &= 2.0\,\text{ms}, \quad \tau_{\text{sd}} = 10.0\,\text{ms}, \quad \tau_{\text{sr}} = 20.0\,\text{ms},\\
s_{\text{K}} &= 0.25\,\text{mV}^{-1}, \quad s_{\text{sd}} = 0.09\,\text{mV}^{-1}, \quad s_{\text{sNa}} = 0.25\,\text{mV}^{-1},\\
\rho &= 0.607, \quad \phi = 0.124, \quad \nu_{\text{acc}} = 0.17, \quad \nu_{\text{dep}} = 0.012,
\end{aligned}
$$

[1] E. K. Miller and T. J. Buschman, Curr. Opin. Neurobiol. **23**, 216 (2013).
[2] R. Follmann, E. E. Macau, E. Rosa, and J. R. Piqueira, IEEE Trans. Neural Netw. Learning Syst. **26**, 1539 (2015).
[3] S. Daan, D. Beersma, and A. A. Borbély, Am. J. Physiol. **246** (Regulatory Integrative Comp. Physiol. 2), R161 (1984).
[4] E. Marder and D. Bucher, Curr. Biol. **11**, R986 (2001).
[5] W. Stein, J. Comp. Physiol. A **195**, 989 (2009).
[6] F. Mormann, T. Kreuz, R. G. Andrzejak, P. David, K. Lehnertz, and C. E. Elger, Epilepsy Res. **53**, 173 (2003).
[7] C. Hammond, H. Bergman, and P. Brown, Trends Neurosci. **30**, 357 (2007).
[8] S. M. Sherman, Trends Neurosci. **24**, 122 (2001).
[9] R. R. Llinás and M. Steriade, J. Neurophysiol. **95**, 3297 (2006).
[10] A. Shilnikov and G. Cymbalyuk, Phys. Rev. Lett. **94**, 048101 (2005).
[11] F. Fröhlich and M. Bazhenov, Phys. Rev. E **74**, 031922 (2006).
[12] M. V. Bennett and R. S. Zukin, Neuron **41**, 495 (2004).
[13] S. Postnova, K. Voigt, and H. A. Braun, J. Biol. Phys. **33**, 129 (2007).
[14] A. L. Hodgkin and A. F. Huxley, J. Physiol. **117**, 500 (1952).
[15] R. Gilmore, X. Pei, and F. Moss, Chaos **9**, 812 (1999).
[16] M. T. Huber and H. A. Braun, Biosystems **89**, 38 (2007).
[17] S. Postnova, E. Rosa, and H. Braun, Pharmacopsychiatry **43**, S82 (2010).
[18] C. Finke, J. A. Freund, E. Rosa, Jr., P. H. Bryant, H. A. Braun, and U. Feudel, Chaos **21**, 047510 (2011).
[19] S. Postnova, P. A. Robinson, and D. D. Postnov, PloS ONE **8**, e53379 (2013).
[20] E. Rosa, Q. M. Skilling, and W. Stein, Biosystems **127**, 73 (2015).
[21] M. Galarreta and S. Hestrin, Proc. Natl. Acad. Sci. USA **99**, 12438 (2002).
[22] Y. Chen, X. Li, H. G. Rotstein, and F. Nadim, J. Neurophysiol., doi:10.1152/jn.00361.2016.
[23] M. van den Top, K. Lee, A. D. Whyment, A. M. Blanks, and D. Spanswick, Nature Neurosci. **7**, 493 (2004).
[24] P. Sah, Trends Neurosci. **19**, 150 (1996).
[25] C. Vergara, R. Latorre, N. V. Marrion, and J. P. Adelman, Curr. Opin. Neurobiol. **8**, 321 (1998).
[26] B. Ermentrout, M. Pascal, and B. Gutkin, Neural Comput. **13**, 1285 (2001).
[27] J. Benda, A. Longtin, and L. Maler, J. Neurosci. **25**, 2312 (2005).
[28] J. P. Roach, L. M. Sander, and M. R. Zochowski, Phys. Rev. E **93**, 052307 (2016).
[29] T. Pereira, J. Eldering, M. Rasmussen, and A. Veneziani, Nonlinearity **27**, 501 (2014).
[30] R. Follmann, E. Rosa, Jr., and W. Stein, Phys. Rev. E **92**, 032707 (2015).
[31] C. Finke, J. A. Freund, E. Rosa, Jr, H. A. Braun, and U. Feudel, Chaos **20**, 045107 (2010).
[32] U. Feudel, A. Neiman, X. Pei, W. Wojtenek, H. Braun, M. Huber, and F. Moss, Chaos **10**, 231 (2000).